

Anomalous Thermal Stability of Metastable C₂₀ Fullerene

I. V. Davydov, A. I. Podlivaev, and L. A. Openov

Moscow Engineering Physics Institute (State University), 115409 Moscow, Russia

ABSTRACT

The results of computer simulation of the dynamics of fullerene C₂₀ at different temperatures are presented. It is shown that, although it is metastable, this isomer is very stable with respect to the transition to a lower energy configuration and retains its chemical structure under heating to very high temperatures, $T \approx 3000$ K. Its decay activation energy is found to be $E_a \approx 7$ eV. Possible decay channels are studied, and the height of the minimum potential barrier to decay is determined to be $U = 5.0$ eV. The results obtained make it possible to understand the reasons for the anomalous stability of fullerene C₂₀ under normal conditions

1. INTRODUCTION

After the discovery of fullerene C_{60} [1], the interest in carbon clusters has greatly increased, due both to their unusual physical and chemical properties and to their prospects for practical applications [2]. In spite of numerous experimental and theoretical studies, the mechanisms of carbon cluster formation and some of their properties are still not clear.

The smallest of the experimentally observed "three-dimensional" carbon clusters is the C_{20} cluster [3], which is one of the fullerenes with a sphere-like structure having carbon atoms located at their "surface" at the vertices of pentagons or hexagons. In fullerene C_{20} , there are only pentagons. A C_{20} cluster can exist both in the form of a fullerene (a cage) and in the form of a bowl, ring, chain, etc. (Fig. 1). The problem of relative stability of these isomers remains to be fully resolved. Experimental data are still incomplete and inconsistent, and theoretical calculations performed using various methods give appreciably different results [4-11]. Partly, this is due to the difficulty in finding the correlation contribution to the total energy of the cluster and also to the fact that the differences in the isomer energies are comparable to the errors of calculation in the methods used.

Nevertheless, most authors who use the most exact modern computing algorithms agree that, of all C_{20} isomers, the bowl has the minimum energy, whereas the cage is a metastable configuration [8, 11]. At the same time, there is no question that, experimentally [3], both C_{20} bowls and C_{20} cages have been synthesized [12, 13]. Thus, there is a question as to why fullerene C_{20} retains an energetically unfavorable chemical structure under real experimental conditions and does not pass to the lower energy configuration.

In this study, the energy and structural characteristics of some C_{20} isomers are calculated using the tight-binding method with a "transferable" potential of interatomic interaction. The

dynamics of fullerene C_{20} is studied in detail at different temperatures. It is shown that, although this three-dimensional isomer is metastable, its lifetime under normal conditions is very long because of a high potential barrier separating the metastable state from the lower energy atomic configuration.

II. METHODS OF CALCULATION

To calculate the energies of different configurations of the C_{20} cluster, we used the tight-binding method with a transferable interatomic potential suggested for carbon compounds in [14]. This method differs favorably from the majority of empirical approaches and allows one to more correctly determine the contribution of the electronic subsystem to the total energy. Thus, four valence electrons of each carbon atom are taken into account and the interatomic potential is actually an N -particle potential, where N is the number of atoms in the system. Although the tight-binding method is not as exact as the *ab initio* methods, it adequately describes both small carbon clusters and macroscopic forms of carbon [7, 14] and, in addition, strongly simplifies calculations even for rather large clusters. In particular, in using the molecular dynamics method, this method makes it possible to collect statistics sufficient for estimating the decay activation energy and the lifetime of the metastable state. Earlier, we applied this method in computer simulation of a metastable C_8 cluster [15-18].

To find equilibrium and metastable configurations of a C_{20} cluster, we used the method of structural relaxation. First, an initial configuration of atoms was chosen, which then relaxed to a state corresponding to a global or local energy minimum under the action of intracuster interactions only. At each time step of the relaxation, the velocities of all atoms were decreased by (1 - 10) %, which is equivalent physically to cooling of the system. The time step was

$t_0 = 2.72 \cdot 10^{-16}$ s, which was approximately equal to one percent of the vibration period for a C_2 dimer.

To determine the decay activation energy of the metastable configuration, we used the method of molecular dynamics with a transferable tight-binding potential (tight-binding molecular dynamics, TBMD [7]) and a time step t_0 . Calculations were performed at a fixed total energy, which corresponds to the case of a heat-insulating system. The temperature T of the cluster was determined from the formula [15]

$$\frac{3}{2}k_B T = \langle E_{kin} \rangle, \quad (1)$$

where k_B is the Boltzmann constant and $\langle E_{kin} \rangle$ is the ion kinetic energy per atom averaged over several vibration periods.

When calculating the forces \mathbf{F}_i acting on the atoms (i is the atom number), we assumed the electron temperature T_{el} to be equal to T and used the formula

$$\mathbf{F}_i = -2 \sum_n \langle \Psi_n | \nabla_i \hat{H} | \Psi_n \rangle f(\varepsilon_n) - \nabla_i U \quad (2)$$

which is a generalization of the Hellmann-Feynman formula to finite temperatures [19, 20]. Here, U is the classical component of the total energy taking into account the repulsion of atoms at close distances; \hat{H} is the electron Hamiltonian in the tight-binding approximation [14]; $|\Psi_n\rangle$ and ε_n are the eigenstates and eigenenergies of \hat{H} , respectively ($n = 1 - 80$); and $f(\varepsilon_n)$ is the Fermi-Dirac distribution function. The chemical potential was determined at each step of molecular dynamics simulation from the condition that the total number of valence electrons was constant, $N_{el} = 80$. To find the effect of the heating of the electron subsystem on the cluster dynamics, we also performed calculations at $T_{el} = 0$.

The height of the potential barrier preventing the transition of the system from the metastable

configuration to a state with a lower energy was calculated by the same method that we used previously in [16]. In this method, calculation reduces to finding the saddle points of the potential energy of the system considered as a function of the coordinates of all atoms. These saddle points correspond to unstable equilibrium positions of atoms in the cluster and possess the property that infinitesimal deviations from the equilibrium positions result either in relaxation of the system to the initial state or in a transition to a new configuration. To find saddle points, the cluster is deformed continuously in the $3N$ -dimensional space of atomic coordinates along the direction of the vibration mode with a minimum frequency so that the cluster energy monotonically increases with deformation, while at the same time having local minima in all others directions (orthogonal to the one chosen) [16].

III. RESULTS

We calculated the structural and energy characteristics of four C_{20} isomers: a cage, a bowl (Fig. 1), a ring, and a chain. For each isomer, the binding energy E_b was calculated from the formula

$$E_b = 20E(C_1) - E(C_{20}) , \quad (3)$$

where $E(C_{20})$ is the binding energy of a C_{20} cluster and $E(C_1)$ is the energy of an isolated carbon atom. The configuration with a maximum energy E_b is stable (equilibrium), since its total energy is minimum. The configurations with smaller (but positive) values of E_b are metastable; they correspond to local minima of the total energy in the space of atomic coordinates.

We obtained the following values of the binding energy E_b per atom: 6.08, 6.14, 5.95, and 5.90 eV/atom for a cage, a bowl, a ring, and a chain, respectively (Table 1). Our results indicate that the C_{20} cage is metastable, which is in agreement with Monte Carlo calculations [8, 11].

The bond lengths between the nearest neighbors in the C₂₀ fullerene are listed in Table 2; these results are in good agreement with the results obtained by other authors.

Heating can transform a metastable isomer to another configuration. The characteristic time of such transformation (the lifetime τ) depends on temperature and the height of the energy barrier separating these configurations. Following general arguments [15], we can see that the cluster decay probability W per unit time is given by the statistics formula

$$W = W_0 \exp(-E_a/k_B T) , \quad (4)$$

where the factor W_0 has dimensions of inverse time (s^{-1}) and E_a is the activation energy for cluster decay. This energy is close to the height of the minimum energy barrier separating the metastable state from the equilibrium state or from another metastable state but can differ from it due to the presence of several different decay paths. The cluster lifetime can be defined as [15]

$$\tau = 1/W = \tau_0 \exp(E_a/k_B T) , \quad (5)$$

where $\tau_0 = 1/W_0$. It is convenient to pass over from the cluster lifetime to the critical number of steps of molecular-dynamics simulation N_c corresponding to cluster decay:

$$N_c = N_0 \exp(E_a/k_B T) , \quad (6)$$

where $N_0 = \tau_0/t_0$.

We performed molecular-dynamics simulation of the "life" of the C₂₀ fullerene at different initial temperatures T of the ionic subsystem; in this way, we directly determined N_c as a function of T . Different values of T corresponded to different sets of initial velocities of the cluster atoms \mathbf{V}_{i0} , which were chosen randomly each time (but subjected to the condition $\sum_i \mathbf{V}_{i0} = 0$).

The results obtained are shown in Fig. 2. Since the nature of the decay of a metastable state is probabilistic, the quantity N_c at a given temperature T is not determined uniquely. Nevertheless, it is seen from Fig. 2 that, in first approximation, the results of simulation are described by Eq. (6), according to which the dependence of $\ln(N_c)$ on $1/T$ is linear. The slope of this line is the activation energy for the cluster decay and is found to be $E_a = 8 \pm 1$ eV at the temperature of the electronic subsystem $T_{el} = T$ and $E_a = 7 \pm 1$ eV at $T = 0$.

Figure 3 shows the results of calculating the "potential landscape" for a C_{20} cluster in the vicinity of the metastable cage configuration (point 1 in Fig. 3). Saddle point 2 is the nearest to the cage state and corresponds to a configuration in which two C-C bonds begin to break and two adjoining octagons form (Fig. 4). The energy of this configuration is 4 eV higher than that of a cage. Analysis of the data of molecular dynamics simulation shows that, though this configuration actually appears from time to time during thermal vibrations, the cluster does not decay. The reason for this behavior is that the energy of the metastable state at point 3, which is the nearest to saddle point 2 (Fig. 3), is only 0.1 eV lower than the energy at the saddle point (visually, atomic configurations 2 and 3 are practically the same; each of them has two octagons). Therefore, after arriving at a new metastable state, the system does not stay there but, due to the thermal motion of atoms, returns (again via saddle point 2) to the vicinity of the initial metastable state at point 1.

Metastable saddle point 4, next to metastable state 3 (Fig. 3), corresponds to a configuration in which two C-C bonds are broken and the breaking of the third bond begins, resulting in the formation of a cluster of three adjoining octagons on the "lateral surface" (Fig. 5). The energy of this configuration is 4.8 eV higher than that of a cage. Metastable state 5, which is the nearest to saddle point 4, also has three octagons (and three broken C-C bonds). Molecular-

dynamics simulation shows that, after passing to metastable state *5*, the system can either return to the vicinity of metastable state *1* via saddle points *4* and *2* or pass to metastable state *7* via saddle point *6* (Fig. 3). In atomic configuration *6*, three C-C bonds are broken and the breaking of another bond begins; because of this, four octagons are formed on the lateral surface of the cluster (Fig. 6). In metastable configuration *7*, there are also four octagons. As a rule, the system does not return from this configuration to the original state *1* (we observed such a return only once). Thus, the difference between the energies of configurations *6* and *1* is the height $U = 5.0$ eV of the minimum potential barrier preventing the cage decay.

Having passed over this barrier and appeared in metastable state *7*, the system, in the overwhelming majority of cases, very rapidly passes via saddle point *8* to metastable state *9* (Fig. 3), where it resides for a time corresponding to $10^3 \div 10^4$ steps of molecular dynamics simulation. Configuration *9* has the form of a star and is shown in Fig. 7. In this symmetric configuration, there are five octagons on the lateral surface of the cluster. The decay of the star leads to the formation of different quasi-two-dimensional or quasi-one-dimensional configurations (Fig. 8) and occurs through transitions via different saddle points (only one of them is shown in Fig. 3). No transition occurs to the equilibrium bowl configuration.

IV. DISCUSSION

It should be noted that the problem of the choice of the temperature of the electron subsystem T_{el} in simulating the dynamics of an electron-ion system is not at all trivial. It is shown in [19] that the use of Eq. (2) in integrating the classical equations of motion for ions corresponds to the conservation of the so-called Mermin free energy [22] $\Omega = E - T_{el}S$, where E is the total internal energy of the system and S is the electronic entropy. Generally, the quantity T_{el}

does not necessarily coincide with the average ionic temperature T [19]. Calculations of the dynamics of different fullerenes at high temperatures performed in [20] showed, in particular, that the stability of the cluster at $T_{el} = T$ appears to be somewhat lower than at $T_{el} = 0$ but that there are no basic qualitative distinctions between these two cases. According to [20], the fragmentation temperature T_{fr} of fullerene C_{20} , defined as the temperature above which the metastable configuration decays, is $T_{fr} \approx 3600$ K and 4000 K at $T_{el} = T$ and $T_{el} = 0$, respectively.

According to our data, the activation energy E_a for the decay of fullerene C_{20} is the same at $T_{el} = T$ and $T_{el} = 0$ to within the limits of error (see Section 3), although the average value of E_a at $T_{el} = T$ is somewhat greater than that at $T_{el} = 0$. Thus, the cluster dynamics weakly depends on the temperature of the electronic subsystem. Partly, this is due to a rather large gap (0.4 eV) between the energies of the lowest unoccupied and the highest occupied molecular orbital (HOMO-LUMO gap). Here, we should emphasize that the "physical time" during which we controlled the dynamics of the C_{20} cluster for each set of initial velocities (i.e., at each initial temperature) exceeded 1.5 ns, which is two orders of magnitude greater than the corresponding time (about 10 ps) in [20, 23], where simulations of the thermal stability of fullerenes were performed. Due to this, we could find the temperature dependence of N_c (i.e., the cluster lifetime) over a fairly large temperature range and estimate the activation energy E_a . Obviously, the lifetime of a metastable state is dependent on temperature. Therefore, it makes no sense to determine (as in [20]) "the temperature of cluster fragmentation" regardless of the time in which this fragmentation occurs.

Using the calculated energy E_a , the lifetime of a C_{20} cage at room temperature, $\tau(300$ K), is found from Eq.(5) to be very large (practically, infinite). This result allows us to understand

the reason for the success of experiments [3] on the synthesis of metastable C_{20} fullerenes. We note that the height of the minimum potential barrier to the decay of a C_{20} cage ($U = 5.0$ eV) is somewhat lower than the decay activation energy $E_a = (6 \div 9)$ eV determined directly from the molecular dynamics simulation data. This is partly due to the fact that the cluster can decay in different ways by passing through potential barriers of different heights, including those that are higher than the lowest barrier.

In [24], calculations of the temperature dependence of the relative root-mean-square fluctuation of bond lengths δ led to the conclusion that the C_{20} cluster melts at a temperature $T_m \approx 1900$ K. According to our calculations, δ monotonically increases with temperature without exhibiting any features at $T < 3000$ K. Moreover, an abrupt cooling of the cluster at any instant prior to its decay results either in its transition to one of the intermediate metastable states (states 3, 5 in Fig. 3) or in its return to the original metastable state (state 1). Thus, the problem of melting of the C_{20} fullerene at a certain temperature T_m requires further study.

Let us now discuss in more detail the character of transition of the C_{20} fullerene to other states. Above all, we note that we never observed a transition to the equilibrium bowl configuration with a lower total energy (higher binding energy). As a rule, the decay of the C_{20} fullerene begins with a transition to the metastable star configuration via a sequence of several saddle points and intermediate short-lived metastable states (Fig. 3). For a star (Fig. 7), the binding energy $E_b = 5.91$ eV/atom is lower than that for a cage. A transition from the cage to the star is accompanied by a decrease in the cluster temperature by (500 - 800) K. Over the course of time, the star passes to different (as a rule, quasi-two-dimensional or quasi-one-dimensional) configurations with a lower binding energy and the cluster temperature decreases from (3000 - 4000) K to (1000 - 1500) K. These configurations are very different in structure

from both the cage and the bowl (one of such configurations is shown in Fig. 8). Thus, the ability of carbon structures to form numerous intermediate metastable (but fairly stable) states prevents the transition of the metastable cage to the stable bowl configuration.

V. CONCLUSIONS

The main result of this study is that the metastable C_{20} fullerene (cage) was demonstrated to have very high thermal stability with respect to transition to an equilibrium state with a lower total energy. The reason for this stability is the high potential barrier, which prevents the decay of the C_{20} cage and the corresponding high decay activation energy. For this reason, the lifetime of the C_{20} cage is very long even at room temperature. Therefore, once created at a certain stage of synthesis, a C_{20} cage retains its chemical structure.

Although all this applies to an isolated C_{20} cage, by analogy to a C_{60} cluster, we may hope that a C_{20} fullerene-based cluster material (fullerite) exists. In any case, the preliminary data are rather encouraging [21, 25, 26]. Final solution of this problem requires further experimental and theoretical studies, one stimulus for which is the conjecture that the C_{20} fullerite (if synthesized) could be a high-temperature superconductor [27].

ACKNOWLEDGMENTS

This study was supported by the CRDF, project "Scientific and Educational Center for Basic Research of Matter in Extremal States".

References

- [1] H. W. Kroto, J. R. Heath, S. C. O'Brien, R. F. Curl, and R. E. Smalley, *Nature* **318**, 162 (1985).

- [2] A. V. Eletskii and B. M. Smirnov, Usp. Fiz. Nauk **165**, 977 (1995) [Phys. Usp. **38**, 935 (1995)].
- [3] H. Prinzbach, A. Weller, P. Landenberger, F. Wahl, J. Worth, L. T. Scott, M. Gelmont, D. Olevano, and B. von Issendorff, Nature **407**, 60 (2000).
- [4] V. Parasuk and A. Almlöf, Chem. Phys. Lett. **184**, 187 (1991).
- [5] D. Bakowies and W. Thiel, J. Am. Chem. Soc. **113**, 3704 (1991).
- [6] D. Tománek and M. A. Schluter, Phys. Rev. Lett. **67**, 2331 (1991).
- [7] C. H. Xu, C. Z. Wang, C. T. Chan, and K. M. Ho, Phys. Rev. B **47**, 9878 (1993).
- [8] J. C. Grossman, L. Mitas, and K. Raghavachari, Phys. Rev. Lett. **75**, 3870 (1995).
- [9] R. O. Jones and G. Seifert, Phys. Rev. Lett. **79**, 443 (1997).
- [10] R. O. Jones, J. Chem. Phys. **110**, 5189 (1999).
- [11] S. Sokolova, A. Lüchow, and J. B. Anderson, Chem. Phys. Lett. **323**, 229 (2000).
- [12] M. Saito and Y. Miyamoto, Phys. Rev. Lett. **87**, 035503 (2001).
- [13] J. Lu, S. Re, Y. Choe, S. Nagase, Y. Zhou, R. Han, L. Peng, X. Zhang, and X. Zhao, Phys. Rev. B **67**, 125415 (2003).
- [14] C. H. Xu, C. Z. Wang, C. T. Chan, and K. M. Ho, J. Phys.: Condens. Matter **4**, 6047 (1992).
- [15] L. A. Openov and V. F. Elesin, Pis'ma Zh. Eksp. Teor. Fiz. **68**, 695 (1998) [JETP Lett. **68**, 726 (1998)]; physics/9811023.

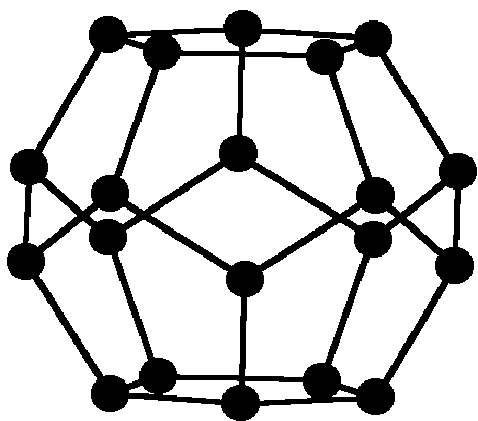
- [16] V. F. Elesin, A. I. Podlivaev, and L. A. Openov, Phys. Low-Dim. Struct. **11/12**, 91 (2000); physics/0104058.
- [17] L. A. Openov and V. F. Elesin, Mol. Mater. **13**, 391 (2000).
- [18] N. N. Degtyarenko, V. F. Elesin, N. E. L'vov, L. A. Openov, and A. I. Podlivaev, Fiz. Tverd. Tela (St. Petersburg) **45**, 954 (2003) [Phys. Solid State **45**, 1002 (2003)].
- [19] R. M. Wentzcovitch, J. L. Martins, and P. B. Allen, Phys. Rev. B **45**, 11 372 (1992).
- [20] B. L. Zhang, C. Z. Wang, C. T. Chan, and K. M. Ho, Phys. Rev. B **48**, 11 381 (1993).
- [21] A. J. Du, Z. Y. Pan, Y. K. Ho, Z. Huang, and Z. X. Zhang, Phys. Rev. B **66**, 035405 (2002).
- [22] N. D. Mermin, Phys. Rev. [Sect. A] **137**, 1441 (1965).
- [23] S. G. Kim and D. Tománek, Phys. Rev. Lett. **72**, 2418 (1994).
- [24] X. Z. Ke, Z. Y. Zhu, F. S. Zhang, F. Wang, and Z. X. Wang, Chem. Phys. Lett. **313**, 40 (1999).
- [25] V. Paillard, P. Mélinon, V. Dupuis, A. Perez, J. P. Perez, G. Guiraud, J. Fornazero, and G. Panczer, Phys. Rev. B **49**, 11433 (1994).
- [26] S. Okada, Y. Miyamoto, and M. Saito, Phys. Rev. B **64**, 245405 (2001).
- [27] I. Spagnolatti, M. Bernasconi, and G. Benedek, Europhys. Lett. **59**, 572 (2002).

Table 1. Binding energies E_b (eV/atom) for some isomers of C_{20} clusters calculated using different methods: tight-binding method (TB), Hartree-Fock method (HF), density functional method in the local density approximation (LDA), density functional method with gradient corrections (GCA), and Tersoff-Brenner empirical method (Tersoff)

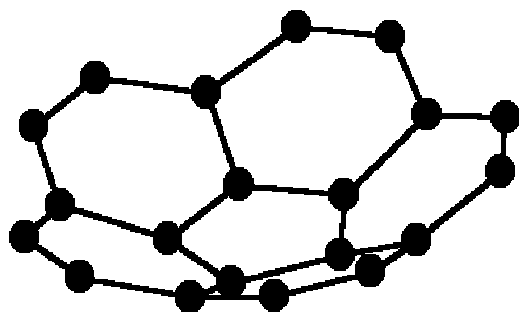
C_{20} isomer	TB [6]	HF [8]	LDA [8]	GCA [9]	Tersoff [21]	This work
Cage	6.08	4.01	7.95	6.36	6.36	6.08
Bowl	-	4.15	7.87	-	6.19	6.14
Ring	6.01	4.23	7.77	6.45	6.11	5.95
Chain	6.05	-	-	6.35	-	5.90

Table 2. Bond lengths in the C_{20} fullerene calculated using different methods: Hartree-Fock method (HF), method of modified neglect of differential overlap (MNDO), and Tersoff-Brenner empirical method (Tersoff)

Method	l_{min} , Å	l_{max} , Å
HF [4]	1.42	1.47
MNDO [5]	1.41	1.52
Tersoff [21]	1.44	1.53
This work	1.44	1.52

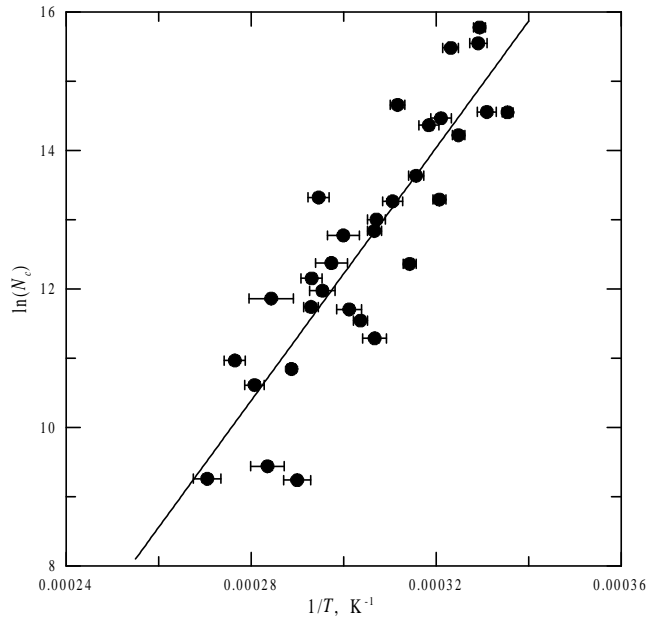


(A)

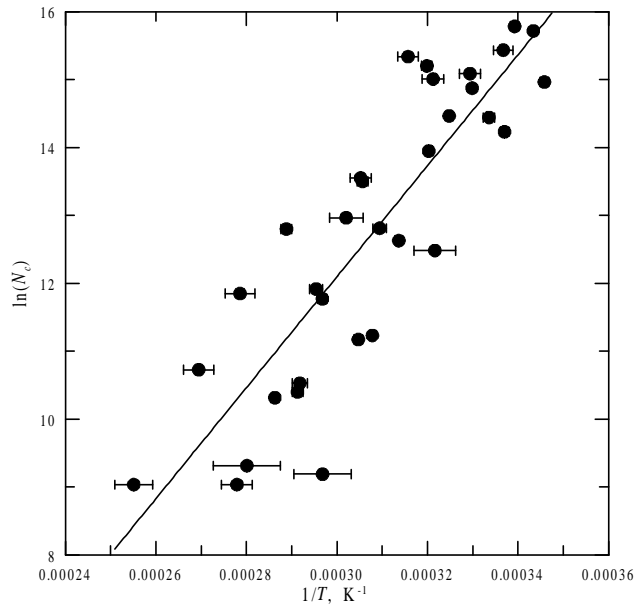


(B)

Fig. 1. Isomers of a C₂₀ cluster. (a) Fullerene (cage) and (b) bowl.



(A)



(B)

Fig. 2. Logarithm of the critical number of steps of molecular dynamics simulation N_c for the onset of the decay of the C_{20} fullerene as a function of the temperature T of the ionic subsystem for electron temperature (a) $T_{el} = T$ and (b) $T_{el} = 0$. Circles are the results of calculation, and

the solid line is a linear least squares fit.

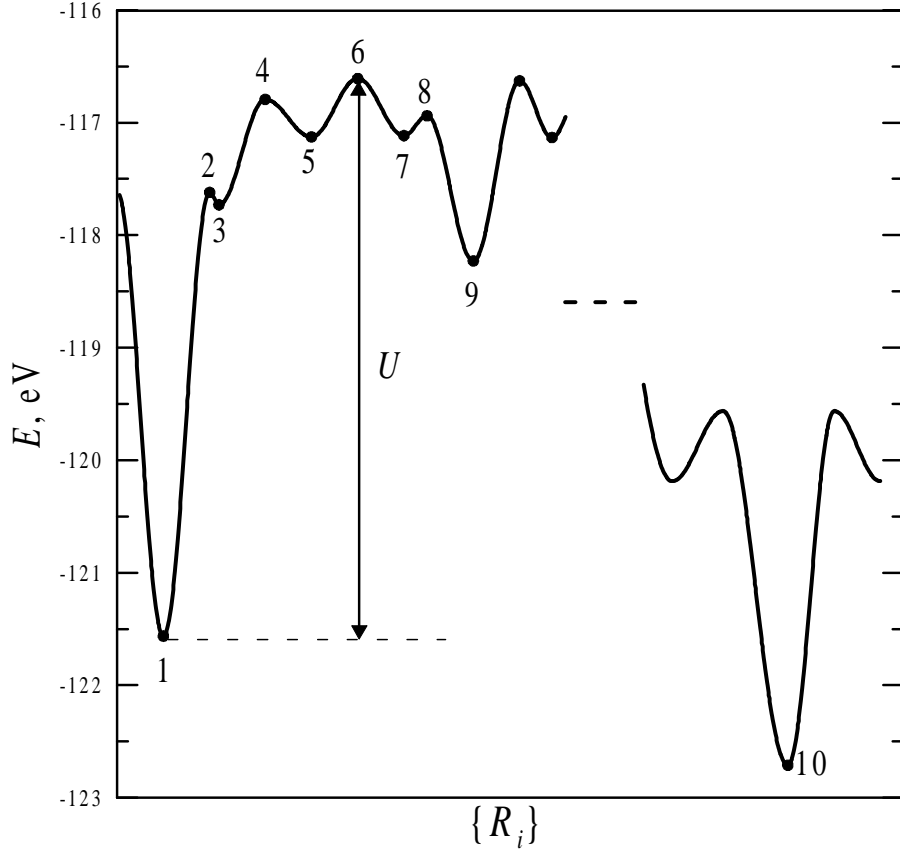


Fig. 3. Dependence of the total energy E of a C_{20} cluster on "the generalized coordinate" in the $3N$ -dimensional space of atomic coordinates \mathbf{R}_i in the vicinity of the metastable cage configuration (schematic). The energies are measured from the energy of 60 isolated carbon atoms. The numerals correspond to the following configurations: (1) fullerene (cage), $E = -121.56$ eV (Fig. 1a); (2) saddle point, $E = -117.62$ eV (Fig. 4); (3) metastable state, $E = -117.73$ eV; (4) saddle point, $E = -116.79$ eV (Fig. 5); (5) metastable state, $E = -117.13$ eV; (6) saddle point determining the height of the minimum potential barrier ($U = 5.0$ eV) to the decay of the cage, $E = -116.61$ eV (Fig. 6); (7) metastable state, $E = -117.12$ eV; (8) saddle point, $E = -116.94$ eV; (9) metastable star state, $E = -118.23$ eV (Fig. 7); and (10) equilibrium bowl configuration, $E = -122.71$ eV (Fig. 1b).

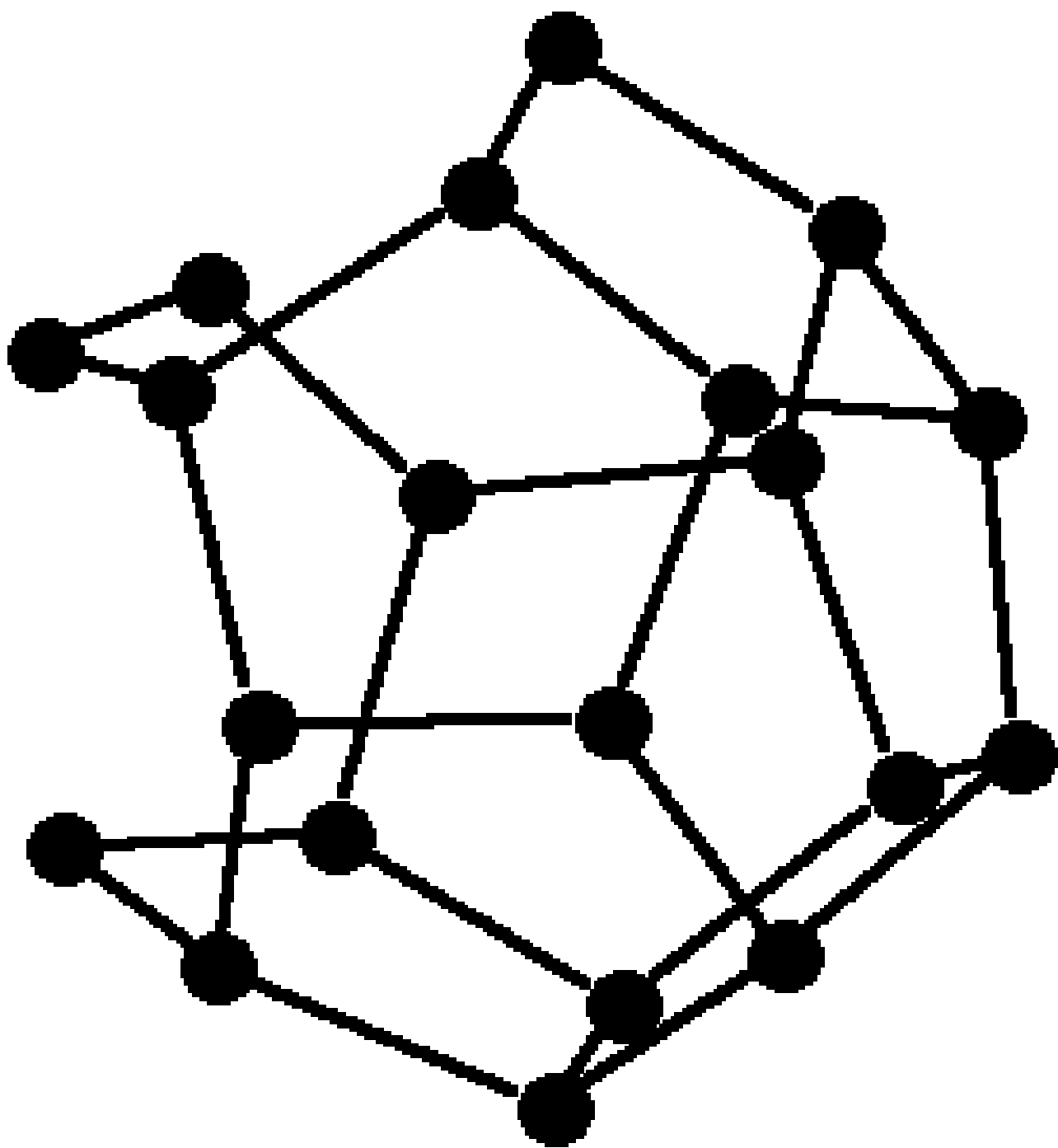


Fig. 4. Atomic configuration corresponding to saddle point 2 in Fig. 3.

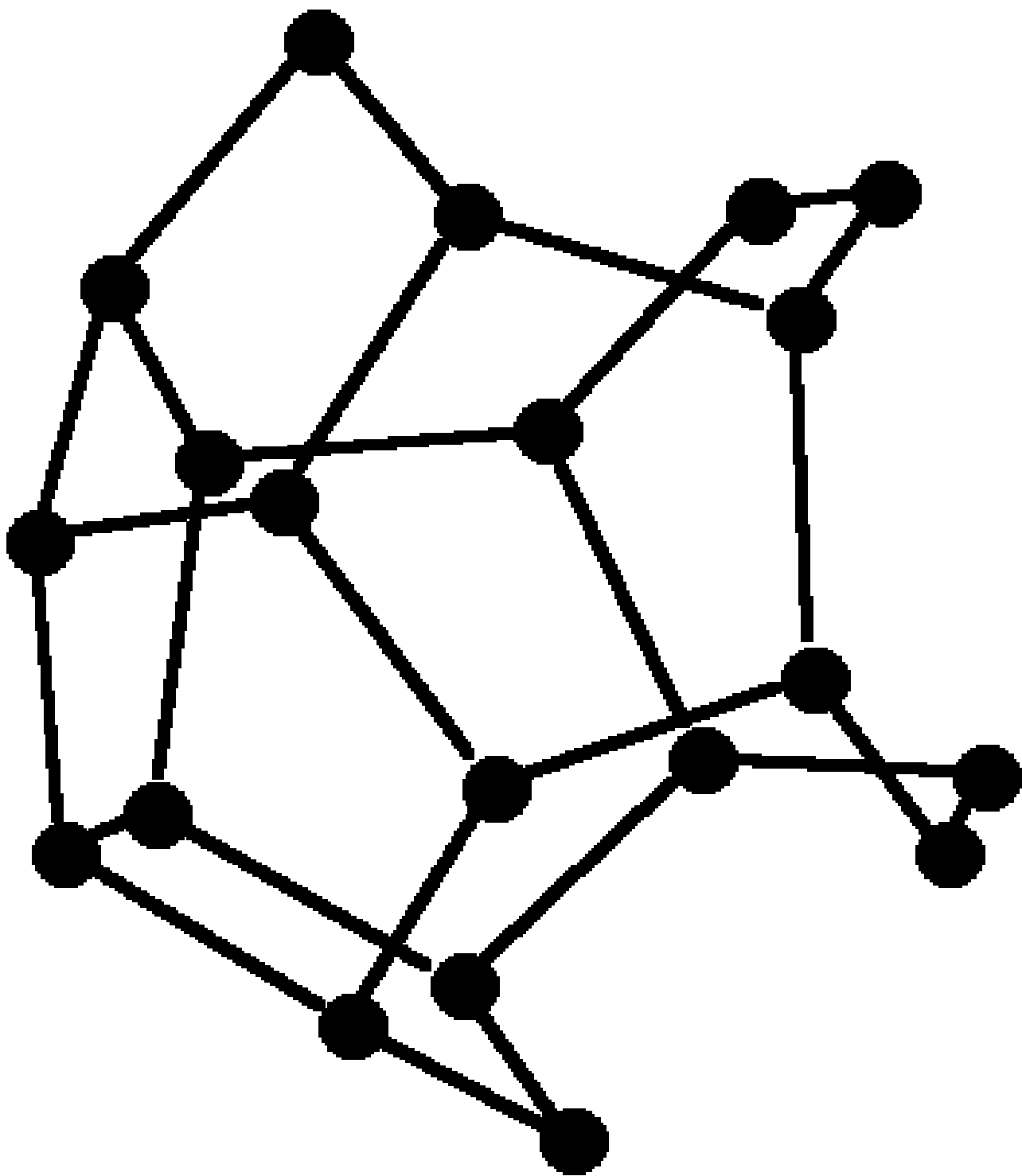


Fig. 5. Atomic configuration corresponding to saddle point 4 in Fig. 3.

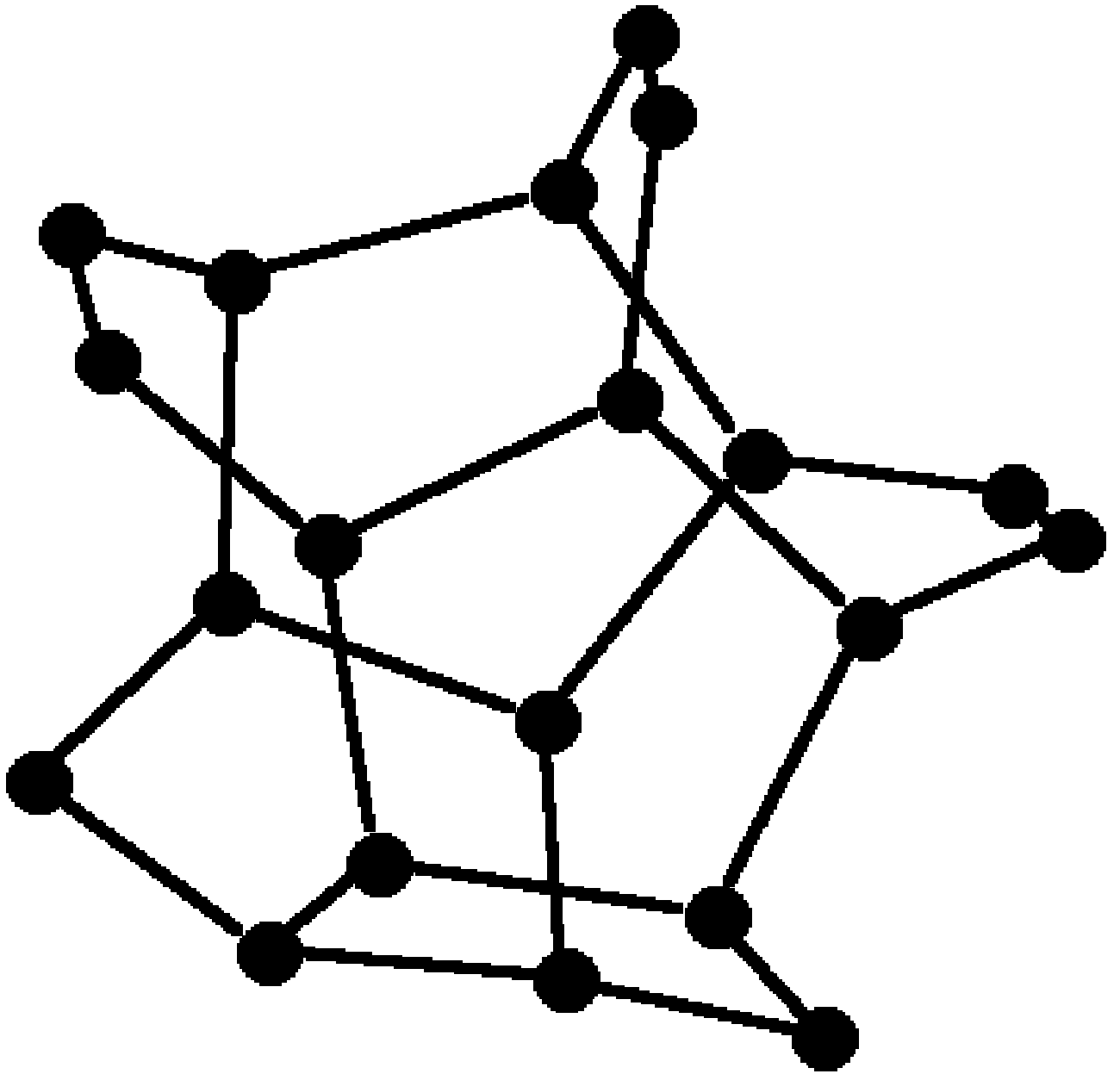


Fig. 6. Atomic configuration corresponding to saddle point 6 in Fig. 3. This configuration determines the height of the minimum potential barrier ($U = 5.0$ eV) to the decay of the cage.

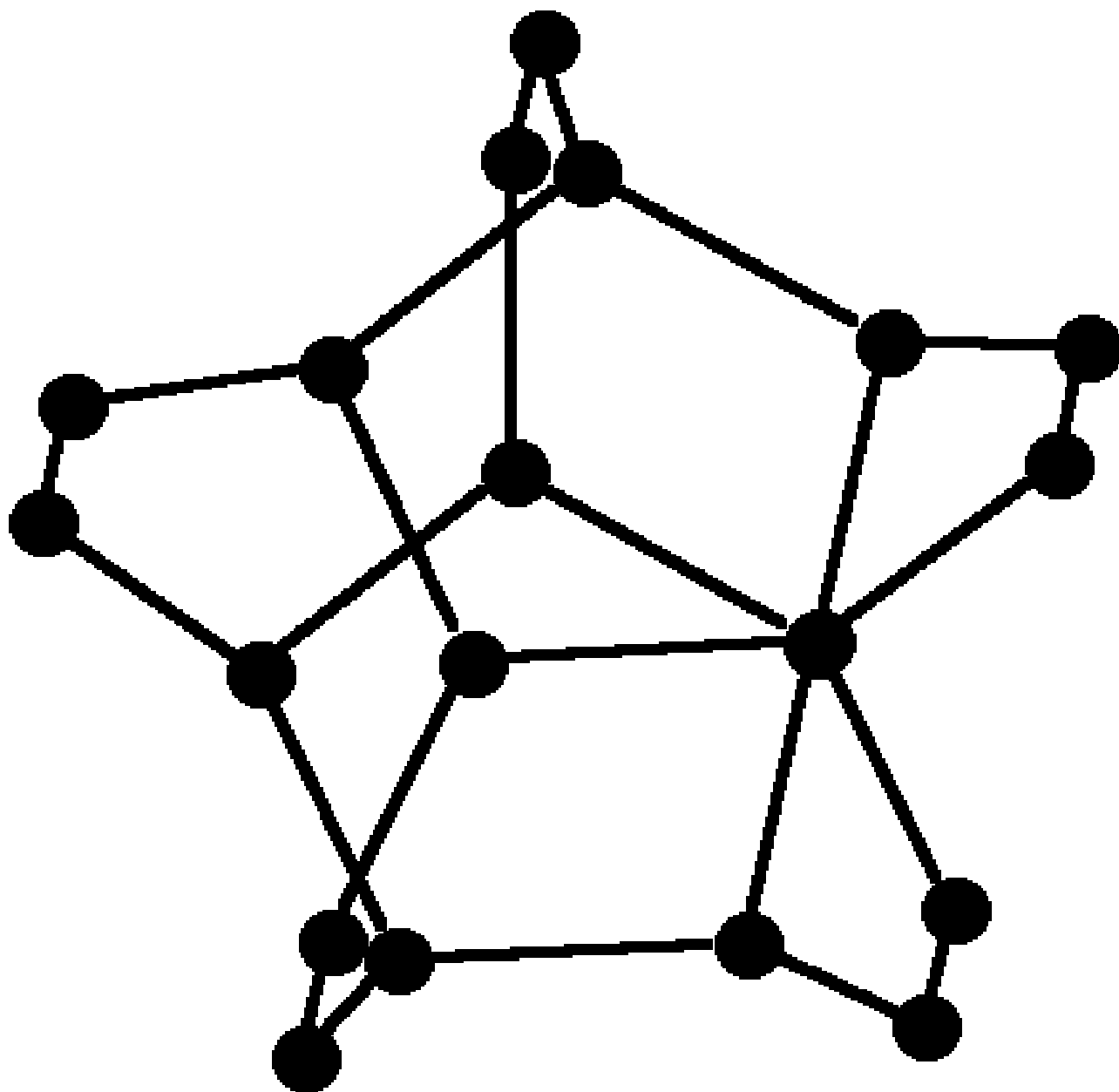


Fig. 7. Atomic configuration "star" corresponding to metastable state 9 in Fig. 3.

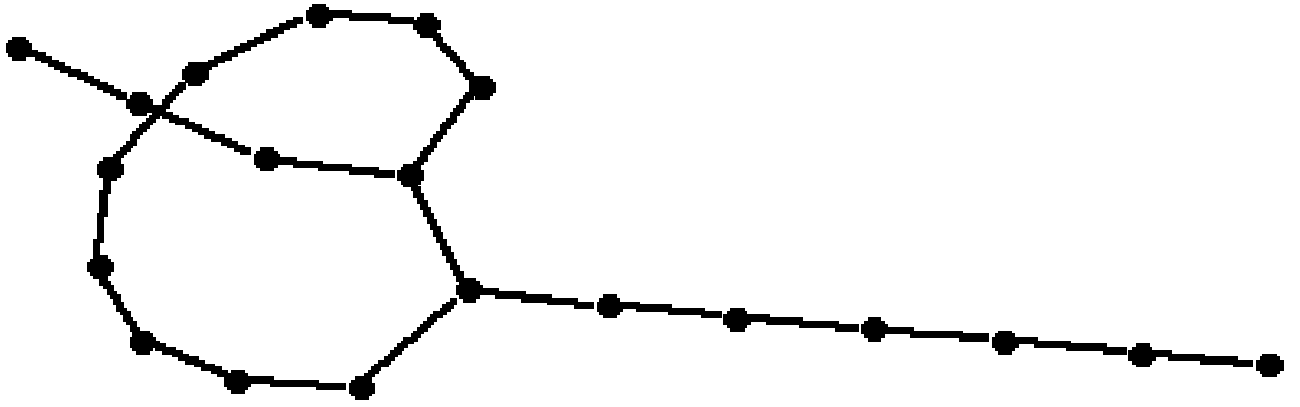


Fig. 8. One of the atomic configurations formed after the decay of the star.